ELSEVIER

Physica B 244 (1998) 114–120

PHYSICA B

Infrared reflectivity of pure and doped $CuGeO_3$

A. Damascelli[a,*], D. van der Marel[a], F. Parmigiani[b], G. Dhalenne[c], A. Revcolevschi[c]

[a] *Solid State Physics Laboratory, University of Groningen, Nijenborgh 4, 9747 AG Groningen, The Netherlands*
[b] *INFM and Dipartimento di Fisica, Politecnico di Milano, Piazza Leonardo da Vinci, 32-20133 Milano, Italy*
[c] *Laboratoire de Chimie des Solides, Université de Paris-sud, Bâtiment 414, F-91405 Orsay, France*

Abstract

We investigated the far- and mid-infrared reflectivity (20–6000 cm^{-1}) of several $Cu_{1-\delta}Mg_{\delta}GeO_3$ ($\delta = 0, 0.01$) and $CuGe_{1-x}Si_xO_3$ ($x = 0, 0.007, 0.05, 0.1$) single crystals. The *b*- and *c*-axis optical response is presented for different temperatures between 4 and 300 K. Moreover, a full group theoretical analysis of the lattice vibrational modes of $CuGeO_3$ in the high-temperature undistorted phase as well as in the low-temperature spin-Peierls phase is reported and compared with the experimental results. We observe the activation of zone boundary phonons along the *b*-axis of the crystal below the spin-Peierls transition temperature. Published by Elsevier Science B.V.

Keywords: $CuGeO_3$; Spin–Peierls transition; Phonons; Far-infrared spectroscopy

1. Introduction

Since $CuGeO_3$ has been recognized, on the basis of magnetic susceptibility measurements [1], as the first inorganic compound showing a spin-Peierls transition (SP), it has attracted the attention of many scientists. In particular, one of the main points of interest was to observe the structural phase transition, occurring in conjunction with the formation of a non-magnetic singlet ground state, both processes being driven by the antiferromagnetic interaction in the one-dimensional Cu–O chains. In fact, many papers on X-ray and neutron-scattering experiments have been published during the last few years, reporting not only the dimerization of the Cu–Cu pairs along the *c*-axis [2], but also the displacement of the Ge and O atoms in the *a–b* plane [3, 4]. Optical techniques are also very useful in investigating magnetic and/or structural phase transitions. Although a considerable amount of Raman scattering [5–7] and infrared spectroscopy [8–10] work has been devoted to the undistorted and the SP phase of $CuGeO_3$, an investigation of the full temperature dependence of the infrared-active phonons has not been reported so far.

In this paper, infrared reflectivity measurements on pure and doped $CuGeO_3$ single crystals, for temperatures ranging from 4 to 300 K, are presented and compared with the results of a group-theoretical analysis performed for the two different crystal structures of $CuGeO_3$.

* Corresponding author. Tel.: + 31 50 363 4922; fax: 363 4825; e-mail; damascel@phys.rug.nl.

0921-4526/98/$19.00 Published by Elsevier Science B.V.
PII S0921-4526(97)00472-9

2. Group-theoretical analysis

At room temperature, $CuGeO_3$ has an orthorhombic crystal structure with lattice parameters $a = 4.81$ Å, $b = 8.47$ Å and $c = 2.941$ Å and space group Pbmm ($x\|a$, $y\|b$, $z\|c$) or, equivalently, Pmma ($x\|b$, $y\|c$, $z\|a$) in standard setting [11]. The building blocks of the structure are edge-sharing CuO_6 octahedra and corner-sharing GeO_4 tetrahedra stacked along the c-axis of the crystal and resulting in Cu^{2+} and Ge^{4+} chains parallel to the c-axis. These chains are linked together via the O atoms and form layers parallel to the b–c plane weakly coupled along the a-axis (Fig. 1). The unit cell contains 2 formula units of $CuGeO_3$ (Fig. 2), with site group C_{2h}^{y} for the 2Cu atoms, C_{2v}^{z} for the 2Ge and the 2O(1) atoms and C_{s}^{xz} for the 4O(2) atoms (where O(2) denotes the O atoms linking the chains together) [3, 4]. A group theoretical analysis can be performed, working in standard orientation, to obtain the number and the symmetry of the lattice vibrational modes. Following the nuclear site group analysis method extended to crystals [12], the contribution of each occupied site to the total irreducible representation of the crystal is

$$\Gamma_{Cu} = A_u + 2B_{1u} + B_{2u} + 2B_{3u},$$

$$\Gamma_{Ge+O(1)} = 2[A_g + B_{1u} + B_{2g} + B_{2u} + B_{3g} + B_{3u}],$$

$$\Gamma_{O(2)} = 2A_g + A_u + B_{1g} + 2B_{1u} + 2B_{2g} + B_{2u} + B_{3g} + 2B_{3u}.$$

Subtracting the silent modes ($2A_u$) and the acoustic modes ($B_{1u} + B_{2u} + B_{3u}$), the irreducible representation of the optical vibrations in standard setting (Pmma), is

$$\Gamma = 4A_g(aa, bb, cc) + B_{1g}(bc) + 4B_{2g}(ab) + 3B_{3g}(ac) + 5B_{1u}(E\|a) + 3B_{2u}(E\|c) + 5B_{3u}(E\|b).$$

This corresponds to an expectation of 12 Raman active modes ($4A_g + B_{1g} + 4B_{2g} + 3B_{3g}$) and 13 infrared active modes ($5B_{1u} + 3B_{2u} + 5B_{3u}$) for $CuGeO_3$, in agreement with the calculation done by Popović et al. [8].

At temperatures lower than T_{SP} the crystal structure is still orthorhombic, but with lattice parameters $a' = 2 \times a$, $b' = b$ and $c' = 2 \times c$ and space group Bbcm ($x\|a$, $y\|b$, $z\|c$) or, equivalently, Cmca ($x\|c$, $y\|a$, $z\|b$) in standard setting [3, 4]. The distortion of the lattice taking place at the phase transition (Fig. 2) is characterized by the dimerization of Cu–Cu pairs along the c-axis (dimerization out of phase in neighboring chains), together with a rotation of the GeO_4 tetrahedra around the axis

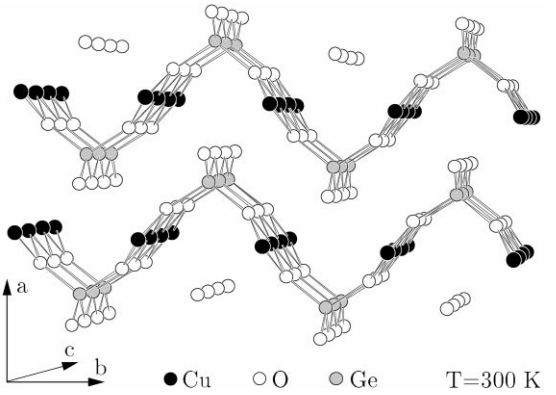

Fig. 1. Crystal structure of $CuGeO_3$ in the high temperature ($T = 300$ K) undistorted phase.

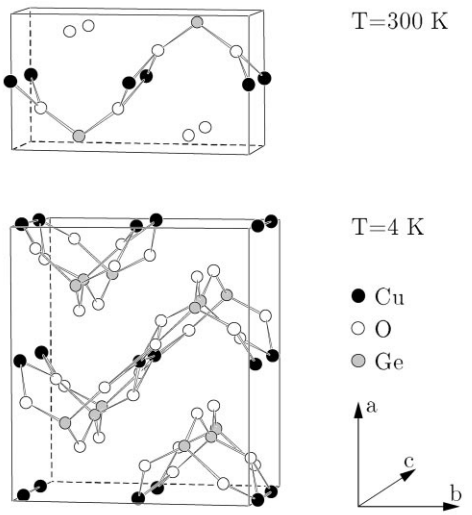

Fig. 2. Conventional unit cell of $CuGeO_3$ in the undistorted (top) and SP phase (bottom). For the purpose of clarity, the ion displacements due to the SP transition have been enlarged by a factor of 30.

defined by the O(1) sites (rotation opposite in sense for neighboring tetrahedra). Moreover, the O(2) sites of the undistorted structure split in an equal number of O(2*a*) and O(2*b*) sites, distinguished by the distances O(2*a*)–O(2*a*) and O(2*b*)–O(2*b*) shorter and larger than O(2)–O(2) [4], respectively. The SP transition is also characterized (Fig. 2) by a doubling of the unit cell (corresponding to a doubling of the degrees of freedom from 30 to 60); the site groups in the new unit cell are: C_2^x for Cu, C_2^y for O(1) and C_s^{yz} for Ge, O(2*a*) and O(2*b*) [4]. Repeating the group-theoretical analysis we obtain for the contributions to the total irreducible representation

$$\Gamma_{Cu} = A_g + A_u + 2B_{1g} + 2B_{1u} + 2B_{2g} + 2B_{2u} + B_{3g} + B_{3u},$$

$$\Gamma_{Ge+O(2a)+O(2b)} = 3[2A_g + A_u + B_{1g} + 2B_{1u} + B_{2g} + 2B_{2u} + 2B_{3g} + B_{3u}],$$

$$\Gamma_{O(1)} = A_g + A_u + 2B_{1g} + 2B_{1u} + B_{2g} + B_{2u} + 2B_{3g} + 2B_{3u}.$$

The irreducible representation of the optical vibrations of $CuGeO_3$ in the SP phase in standard setting (Cmca), is

$$\Gamma_{SP} = 8A_g(aa, bb, cc) + 7B_{1g}(ac) + 6B_{2g}(bc) + 9B_{3g}(ab) + 9B_{1u}(E\|b) + 8B_{2u}(E\|a) + 5B_{3u}(E\|c).$$

Therefore, 30 Raman active modes ($8A_g + 7B_{1g} + 6B_{2g} + 9B_{3g}$) and 22 infrared active modes ($9B_{1u} + 8B_{2u} + 5B_{3u}$) are expected for $CuGeO_3$ in the SP phase, all the additional vibrations being zone boundary modes activated by the folding of the Brillouin zone.

To compare the results obtained for the undistorted and the SP phase of $CuGeO_3$, it is better to rewrite the irreducible representations Γ and Γ_{SP} into Pbmm and Bbcm settings, respectively, because both groups are characterized by: $x\|a$, $y\|b$ and $z\|c$. This can be done by permuting the (1g, 2g, 3g) and (1u, 2u, 3u) indices in such a way that it corresponds to the permutations of the axis relating Pmma to Pbmm and Cmca to Bbcm. Therefore, the irreducible representations of the optical vibrations of $CuGeO_3$, for $T > T_{SP}$ (Pbmm) and $T < T_{SP}$ (Bbcm), respectively, are

$$\Gamma' = 4A_g(aa, bb, cc) + 4B_{1g}(ab) + 3B_{2g}(ac) + B_{3g}(bc) + 3B_{1u}(E\|c) + 5B_{2u}(E\|b) + 5B_{3u}(E\|a),$$

$$\Gamma'_{SP} = 8A_g(aa, bb, cc) + 9B_{1g}(ab) + 7B_{2g}(ac) + 6B_{3g}(bc) + 5B_{1u}(E\|c) + 9B_{2u}(E\|b) + 8B_{3u}(E\|a).$$

It is now evident that the number of infrared active phonons is expected to increase from 5 to 8, 5 to 9 and 3 to 5 for light polarized along the *a*-, *b*- and *c*-axis, respectively.

3. Experimental

We investigated the far- and mid-infrared reflectivity (20–6000 cm^{-1}) of several $Cu_{1-\delta}Mg_\delta GeO_3$ ($\delta = 0, 0.01$) and $CuGe_{1-x}Si_xO_3$ ($x = 0, 0.007, 0.05, 0.1$) single crystals. These high-quality single crystals were grown from the melt by a floating-zone technique [13]. Samples with dimensions of $1 \times 3 \times 6\ mm^3$ were aligned by conventional Laue diffraction and mounted in a liquid-He flow cryostat to study the temperature dependence of the optical properties between 4 and 300 K. The reflectivity measurements were performed with a Fourier transform spectrometer (Bruker IFS 113v), operating in near-normal incidence configuration with polarized light in order to probe the optical response of the crystals along the *b*- and the *c*-axis. The absolute reflectivities were obtained by calibrating the data acquired on the samples against a gold mirror.

4. Results

4.1. Pure $CuGeO_3$

The *c*- and *b*-axis reflectivity spectra of $CuGeO_3$ in the undistorted phase are shown in Fig. 3, for two different temperatures. The data are shown up to 1000 cm^{-1} which covers the full phonon

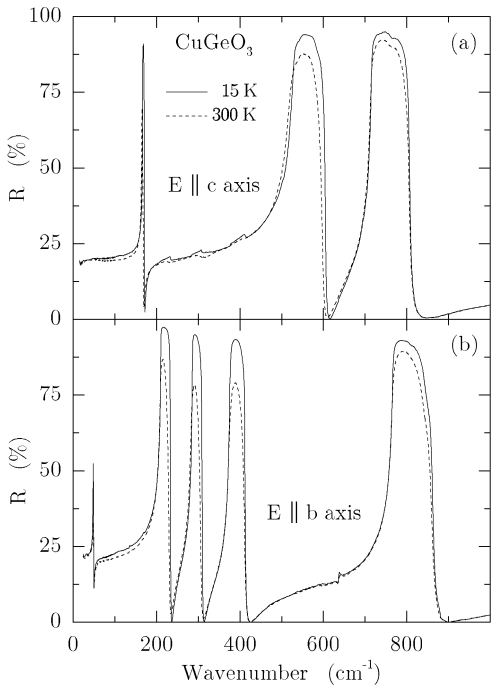

Fig. 3. Reflectivity of a single crystal of pure $CuGeO_3$ as a function of wave number at two different temperatures (300 and 15 K) in the undistorted phase. The spectra are shown for light polarized along the *c*-axis (a), and the *b*-axis (b) of the crystal.

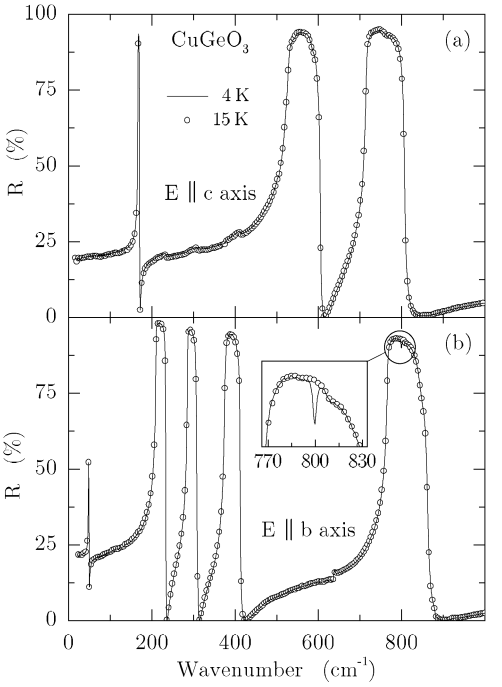

Fig. 4. Comparison between reflectivity spectra measured in the SP phase at 4 K (solid line) and just before the SP transition at 15 K (circles) on a pure single-crystal of $CuGeO_3$. For light polarized along the *c*-axis (a) no difference is found across the phase transition whereas for light polarized along the *b*-axis (b) a new feature appears at 800 cm^{-1} (as clearly shown in the inset).

spectrum. The spectra are typical of an insulating material. Three phonons are detected along the *c*-axis ($\omega_{TO} \approx 167$, 528 and 715 cm^{-1} for $T = 15$ K), and five along the *b*-axis ($\omega_{TO} \approx 48, 210$, 286, 376 and 766 cm^{-1} for $T = 15$ K), in agreement with the calculation presented in Section 2. The structure in Fig. 3(a) between 200 and 400 cm^{-1} is due to a leakage of the modes polarized along the *b*-axis and the feature at approximately 630 cm^{-1} in Fig. 3(b) is a leakage of a mode polarized along the *a*-axis [8].

In Fig. 4 the reflectivity measured at 4 K in the SP phase is compared with the data obtained just above $T_{SP} = 14$ K. Whereas for $E \| c$ the spectra are exactly identical, a new feature is detected in the SP phase at 800 cm^{-1} for $E \| b$, as clearly shown in the inset of Fig. 4(b). This line (that falls in the frequency region of high reflectivity for the phonon at 766 cm^{-1} and therefore shows up mainly for its absorption) can be, in our opinion, interpreted as a folded mode due to the SP transition. The reason for not observing all phonons predicted from the group theoretical analysis is probably the small value of the atomic displacements involved in the SP transition, with a correspondingly small oscillator strength of zone boundary phonons.

4.2. *Doped $CuGeO_3$*

The reflectivity data acquired on the Si-doped samples for $E \| c$ and $E \| b$ are shown in Figs. 5 and 6, respectively. Some new features, due only to the substitution of Ge with the lighter Si and not directly related to the SP transition, are observable: new phonon peaks at 900 cm^{-1} along the *c*-axis

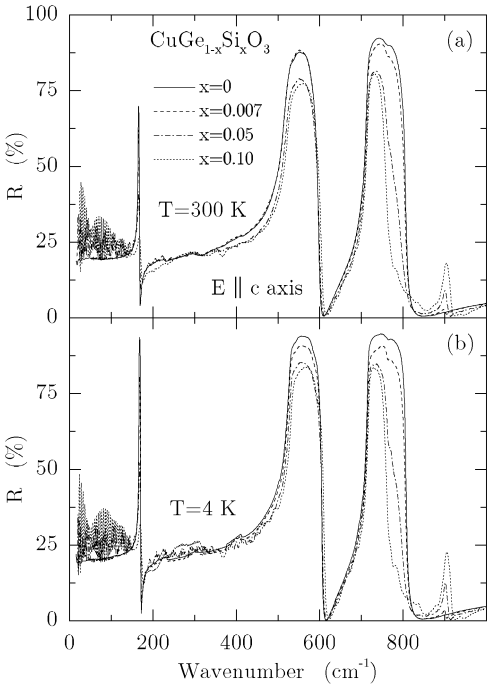

Fig. 5. *C*-axis reflectivity of Si-doped single crystals of $CuGeO_3$ for different silicon concentrations. The spectra are presented as a function of wave number for $T = 300$ K (a) and $T = 4$ K (b).

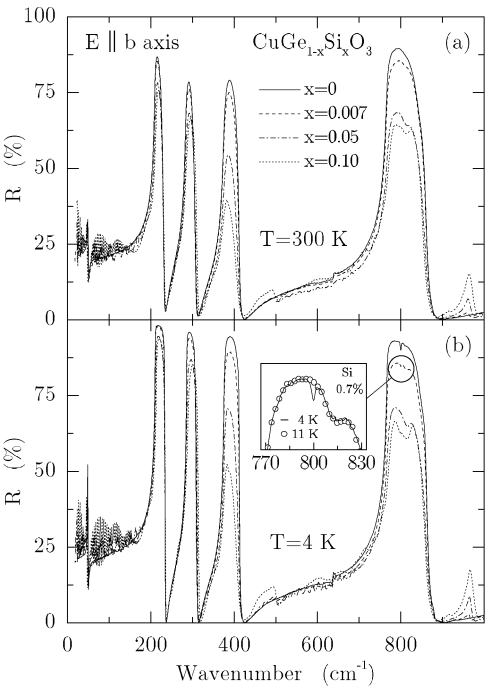

Fig. 6. *B*-axis reflectivity of Si-doped single crystals of $CuGeO_3$ for different silicon concentrations. The spectra are presented as a function of wave number for $T = 300$ K (a) and $T = 4$ K (b). The 800 cm^{-1} excitation activated by the SP transition is still observable for 0.7% Si-doping by comparing (see inset) the 4 K (solid line) and the 11 K (circles) data.

(Fig. 5) and at 500 and 960 cm^{-1} along the *b*-axis (Fig. 6). Moreover, the more complicated line shape and the reduction of the oscillator strength of the high-frequency phonons indicate a strong Ge (Si) contribution to these modes, mainly due to O vibrations. At low temperatures we observe the mode at 800 cm^{-1} for $E\|b$ only for the lowest Si concentration, as shown in the inset of Fig. 6(b), where the 4 and 11 K data are compared. We conclude that up to 0.7% Si doping the SP transition is still present with $T_{SP} < 11$ K, whereas for 5% and 10% Si concentrations no indication of the transition could be found in our spectra.

The results obtained on the Mg-doped sample are plotted in Figs. 7 and 8 for $E\|c$ and $E\|b$, respectively. Clearly, Mg doping affects the optical response of $CuGeO_3$ less than Si doping. A new phonon due to the mass difference between Cu and Mg is present in the *c*-axis spectra at 695 cm^{-1}, as clearly shown in the inset of Fig. 7(b), for $T = 4$ K. Moreover, we clearly observe for $E\|b$ [see inset of Fig. 8(b)], the 800 cm^{-1} feature related to the SP transition. On the one hand, for the 1% Mg-doped sample, T_{SP} seems to be lower than in pure $CuGeO_3$; on the other hand, the structural deformation is not as strongly reduced as in the 0.7% Si-doped sample, as can be deduced from the comparison between the insets of Fig. 6(b) and Fig. 8(b).

5. Conclusions

In summary, we have investigated the infrared reflectivity of pure and Mg- and Si-doped $CuGeO_3$ single crystals, for *E* polarized parallel to the *b*- and

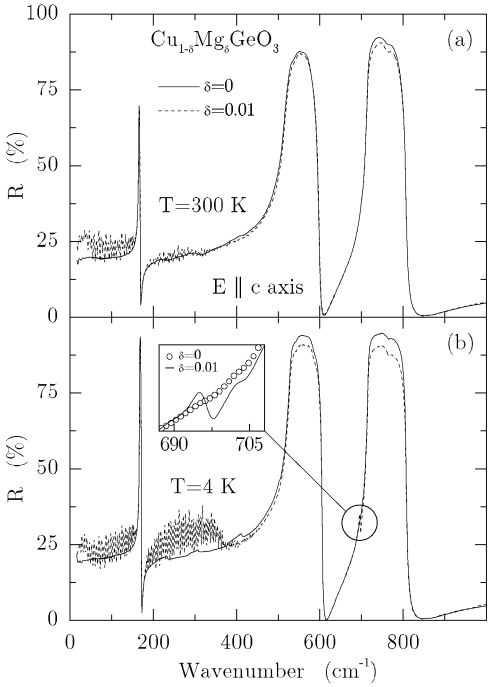

Fig. 7. *C*-axis reflectivity of pure and 1% Mg-doped single crystals of $CuGeO_3$. The spectra are presented as a function of wave number for $T = 300$ K (a) and $T = 4$ K (b). The inset shows an enlarged view of the frequency region around 700 cm^{-1} for the data obtained on the pure (circles) and Mg-doped (solid line) samples, at $T = 4$ K. The additional peak observed for Mg doping is due to the mass difference between Cu and Mg and it is not related to the SP transition.

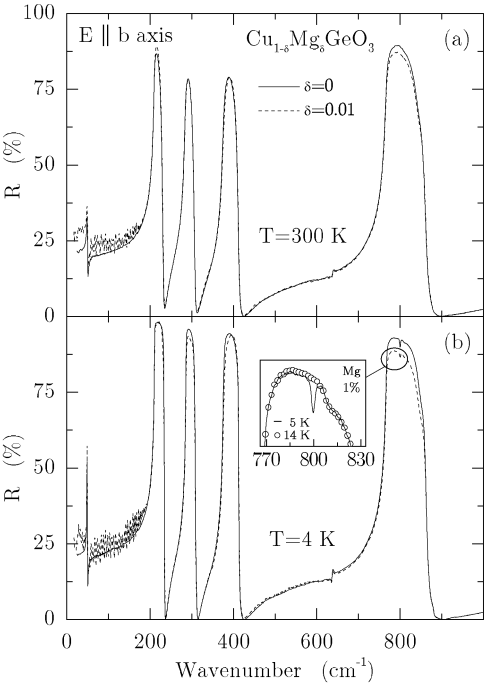

Fig. 8. *B*-axis reflectivity of pure and 1% Mg-doped single crystals of $CuGeO_3$. The spectra are presented as a function of wave number for $T = 300$ K (a) and $T = 4$ K (b). For the Mg-doped sample the 800 cm^{-1} excitation activated by the SP transition is clearly observable in the inset, where the 4 K (solid line) and the 14 K (circles) data are presented.

c-axis of the crystals and temperatures ranging from 4 to 300 K. The results of a group-theoretical calculation for the undistorted and distorted structures of $CuGeO_3$ are presented and compared with the experimental data. A feature reflecting the SP transition has been observed in the phonon spectrum and interpreted as a folded zone boundary mode.

Acknowledgements

We gratefully acknowledge M. Mostovoi and D.I. Khomskii for stimulating discussions. We thank K. Schulte, A.-M. Janner and M. Grüninger for many useful comments and Z. Tomaszewski for technical help. This investigation was supported by the Netherlands Foundation for Fundamental Research on Matter (FOM) with financial aid from the Nederlandse Organisatie voor Wetenschappelijk Onderzoek (NWO).

References

[1] M. Hase, I. Terasaki, K. Uchinokura, Phys. Rev. Lett. 70 (1993) 3651.
[2] J.P. Pouget, L.P. Regnault, M. Aïn, B. Hennion, J.P. Renard, P. Veillet, G. Dhalenne, A. Revcolevschi, Phys. Rev. Lett. 72 (1994) 4037.
[3] K. Hirota, D.E. Cox, J.E. Lorenzo, G. Shirane, J.M. Tranquada, M. Hase, K. Uchinokura, H. Kojima, Y. Shibuya, I. Tanaka, Phys. Rev. Lett. 73 (1994) 736.
[4] M. Braden, G. Wilkendorf, J. Lorenzana, M. Aïn, G.J. McIntyre, M. Behruzi, G. Heger, G. Dhalenne, A. Revcolevschi, Phys. Rev. B 54 (1996) 1105.

[5] H. Kuroe, T. Sekine, M. Hase, Y. Sasago, K. Uchinokura, H. Kojima, I. Tanaka, Y. Shibuya, Phys. Rev. B 50 (1994) 16468.
[6] S. Jandl, M. Poirier, M. Castonguay, P. Fronzes, J.L. Musfeldt, A. Revcolevschi, G. Dhalenne, Phys. Rev. B 54 (1996) 7318.
[7] A.R. Goñi, T. Zhou, U. Schwarz, R.K. Kremer, K. Syassen, Phys. Rev. Lett. 77 (1996) 1079.
[8] Z.V. Popović, S.D. Dević, V.N. Popov, G. Dhalenne, A. Revcolevschi, Phys. Rev. B 52 (1995) 4185.
[9] N.E. Massa, J. Campá, I. Rasines, Phys. Rev. B 52 (1995) 15920.
[10] P.H.M. van Loosdrecht, S. Huant, G. Martinez, G. Dhalenne, A. Revcolevschi, Phys. Rev. B 54 (1996) R3730.
[11] H. Völlenkle, A. Wittmann, H. Nowotny, Monatsh. Chem. 98 (1967) 1352.
[12] D.L. Rousseau, R.P. Bauman, S.P.S. Porto, J. Raman Spectrosc. 10 (1981) 253.
[13] A. Revcolevschi, G. Dhalenne, Adv. Mater. 5 (1993) 657.